Enhanced Minijet Production in $A - A$ Collisions from Gluons with Large Transverse Momenta

H.-J. Pirner and Feng Yuan

Institut für Theoretische Physik, Universität Heidelberg, Philosophenweg 19, 69120 Heidelberg,

Germany

(January 2001)

Abstract

We find supersaturation for the intrinsic gluon distribution of nuclei, i.e. the low x unintegrated nuclear gluon distribution peaks at intermediate transverse momenta $k_t = Q_s$ and vanishes at zero k_t. Taking into account the intrinsic transverse momenta of the gluons and the saturation scale p_s of the produced gluons, we calculate the minijet cross section arising from gluon gluon scattering for RHIC energies. For central collisions at $\sqrt{s} = 200 GeV$ the saturation scale $p_s \approx 1.4$ GeV is larger due to intrinsic k_t effects and increases with energy. Our theoretical results on charged particle multiplicity agree very well with the recent experimental data from RHIC.

PACS number(s): 24.85.+p,25.75.+r,12.38.Bx

Typeset using REVTEX

I. INTRODUCTION

With the operation of RHIC [1–3], heavy ion collisions have entered a new era, where semihard collisions become more important compared to soft collisions . Therefore a detailed knowledge of intrinsic parton distributions is important for a quantitative understanding of heavy quark production and/or cross sections at large transverse momenta. Due to the increase of the gluon distribution at small x, a sizeable cross section at mid rapidity comes from the region where the transverse momenta of partons become comparable to their longitudinal momenta. Therefore a k_t factorization scheme is preferred, where the intrinsic transverse momenta of partons are included in the calculation of the minijet cross sections. Especially in nuclei, intrinsic transverse momenta of gluons can become quite large, since at small x the gluon clouds of the individual nucleons overlap and interact accumulating large transverse momenta. A careful inversion of the color dipole nuclear cross section allows to assess this effect.

We differentiate between the gluon saturation scale Q_s due to the interaction of gluons with one another inside the same nucleus *before* the collision and the saturation scale p_s of produced gluons *after* the first collision between the nuclei. Both scales arise due to different mechanisms, but sometimes appear to be of the same magnitude.

Inside the nucleus supersaturation occurs due to the color neutrality of the nucleons. One cannot have gluons at small x and small k_t, because the nucleons from which they originate are color neutral. This finding is derived from a careful inversion of the multiple scattering of a test color dipole on the nucleus. It is confirmed by the evaluation of the BFKL equation in the nucleus [4]. We will give our derivation of the unintegrated gluon distribution in nuclei in section II.

In section III we will use this distribution to calculate the mini jet cross section $g + g \rightarrow g + g$. Due to the intrinsic transverse momenta of the gluons the LO QCD cross section is enhanced at a given cut off scale. Since the intrinsic transverse momenta depend on the number of gluon clouds overlapping, we find that for more central collisions the enhancement

is larger.

Section IV is devoted to the analysis of the gluon system which is produced after the first collision. These now on shell gluons are numerous at small nuclear impact parameters and crowd the impact parameter dependent area $F(b)$ of intersection between the two nuclei. Concentrating on gluons in the central rapidity region one sees that their number $\frac{dN}{dy}$ times their individual size π/p_s^2 cannot exceed the area $F(b)$. This equation comes from an estimate of the number of merging gluons $2 \rightarrow 1$ of produced gluons compared to the number of splitting gluons $1 \rightarrow 2$ [5,6]. Since the number of gluons decreases severely as $1/p_s^2$ and the saturation criterion $F(b) \times p_s^2$ increases with p_s^2 one obtains a self consistent determination of the saturation scale of produced partons p_s [7]. Intrinsic transverse momentum will increase the number of produced gluons at the same cut off. As a final result, these effects lead to a higher saturation scale $p_s \approx 1.5\text{GeV}$ than the scale found without intrinsic k_t. In the framework of local parton hadron duality the so derived gluon distribution can be directly applied to estimate the number of produced charged hadrons. From e^+e^- collisions [8] the conversion factor is known and of order unity. In this section, we will also present the prediction on charged particle multiplicity based on our saturation criterion. As first pointed in [9], the centrality dependence of charged particle multiplicity can be used to test different saturation models. And very recently, there have been several studies on this quantity by using different saturation approaches [10,11]. We will find the saturation criterion we used in the following gives reasonable description on centrality dependence of charged particle reported by PHENIX collaboration [3].

In section V we give a summary of our results and discuss the possibility to determine the intrinsic saturation scale Q_s by measuring "monojets".

II. UNINTEGRATED GLUON DISTRIBUTIONS IN COLD NUCLEI

We know that the dipole-proton cross section depends on the unintegrated gluon distribution function $f_g(x, k_t^2)$. Assuming a perturbative 2 gluon exchange picture one has the

following equation for a color neutral dipole with transverse size r, virtuality Q^2 and energy $s = (Q^2 + m_\rho^2)/x$. We assume α_s fixed, [12]

$$\hat{\sigma}_{d-p}(s, r) = \frac{4\pi}{3} \int \frac{d^2 k_t}{k_t^2} [1 - e^{i\vec{r} \cdot \vec{k_t}}] \alpha_s f_g(x, k_t^2). \tag{1}$$

Here $f_g(x, k_t^2)$ is the unintegrated gluon distribution of the proton, which is related to the normal integrated gluon density as

$$xG(x, Q^2) = \int^{Q^2} dk_t^2 f_g(x, k_t^2). \tag{2}$$

The unintegrated gluon distribution function can be obtained from the color dipole-proton cross section $\hat{\sigma}_{d-p}$ in Eq. (1) by inversion. Since the cross section contains the color dipole factor $[1 - e^{i\vec{r} \cdot \vec{k_t}}]$, the inversion is more complicated than a Fourier Bessel transform. The energy of the dipole cross section under the integrand depends on the virtuality k_t^2 as $s = (k_t^2 + m_\rho^2)/x$.

$$\alpha_s f_g(x, k_t^2) = \frac{3}{16\pi^3} k_t \frac{d}{dk_t} k_t \frac{d}{dk_t} \int \frac{d^2 r}{r^2} J_0(k_t r) \hat{\sigma}_{d-p}(x, r)$$

$$= \frac{3}{16\pi^3} \int \frac{d^2 r}{r^2} [-k_t r J_1(k_t r) - \frac{k_t^2 r^2}{2} (J_0(k_t r) - J_2(k_t r))] \times \hat{\sigma}_{d-p}(s, r), \tag{3}$$

where J_0, J_1, and J_2 are Bessel functions.

We can derive the unintegrated gluon distribution function in nuclei by using the same method. The cross section of a test color dipole on the nucleus A depends on the nuclear thickness function $T(b)$. For a hard sphere nucleus we would have $T(b) = 2\rho_0 \sqrt{R_A^2 - b^2}$ with $\rho_0 = 0.16 fm^{-3}$. For the following calculations, however, we always use realistic thickness functions obtained from a nuclear density distribution with finite thickness. This is important for peripheral collisions. According to Glauber theory the total nuclear cross section has the following form:

$$\hat{\sigma}_{d-A}(x, r) = \int d^2 b \hat{\sigma}_{d-A}(b, x, r), \tag{4}$$

$$\hat{\sigma}_{d-A}(b, x, r) = 2(1 - e^{-\frac{1}{2} T(b) \hat{\sigma}_{d-p}(s, r)}). \tag{5}$$

The differential cross section $\sigma_{d-A}(b, x, r)$ with respect to the nuclear impact parameter b is related to the unintegrated gluon distribution $f_{g/A}(x, k_t, b)$ in the nucleus at impact parameter b.

$$\hat{\sigma}_{d-A}(b, x, r) = \frac{4\pi}{3} \int d^2 b \frac{d^2 k_t}{k_t^2} [1 - e^{i\vec{r}\cdot\vec{k_t}}] \alpha_s f_{g/A}(x, k_t, b), \tag{6}$$

which yields the normal gluon distribution in the nucleus after integration.

$$xG_A(x, Q^2) = \int^{Q^2} dk_t^2 d^2 b f_{g/A}(x, k_t, b). \tag{7}$$

From Eqs. (4) and (6), we can derive the unintegrated gluon density of nucleus A as,

$$\alpha_s f_{g/A}(x, k_t, b) = \frac{3}{16\pi^3} \int \frac{d^2 r}{r^2} [-k_t r J_1(k_t r) - \frac{k_t^2 r^2}{2}(J_0(k_t r) - J_2(k_t r))] \times 2(1 - e^{-\frac{1}{2}T(b)\hat{\sigma}_{d-p}(s,r)}). \tag{8}$$

One sees that in the limit of small density the integrated density in the nucleus would be A times as big as in the proton (shadowing effects will give some modifications). To obtain the unintegrated gluon density of nuclei from the above equations, we must know the parameterization of the dipole cross section $\hat{\sigma}_{d-p}(r)$. Up to now, there are various parameterizations for this function [13–15]. As a rough estimate, we use the following simple parameterization,

$$\hat{\sigma}_{d-p}(r) = C(0, s)r^2. \tag{9}$$

We take the energy dependent coefficient $C(0, s)$ from the parameterization of Ref. [15],

$$C(0, s) = \sigma_0(s)/R_0^2(s), \tag{10}$$

where the parameterizations for $\sigma_0(s)$ and $R_0(s)$ can be found in [15]. To compensate other effects (e.g. shadowing [16]), we normalize our unintegrated gluon density to the integrated gluon density according to Eq. (7) for $Q^2 \gg Q_s^2$. Finally, we get the following results for the double differential gluon distribution, (cf. Fig. 1)

$$f_{g/A}(x, k_t, b) = T(b) \times xG_A(x) \frac{k_t^2}{(Q_s^2)^2} e^{-\frac{k_t^2}{Q_s^2}}, \tag{11}$$

where

$$Q_s^2 = 2T(b) \times C(0, s), \tag{12}$$

Note that the intrinsic momentum distribution depends on the closeness to the center of the nucleus. The smaller b the more gluon clouds in the nucleus overlap producing a larger gluon transverse momentum. At central $b = 0$ the mean transverse momentum in the gluons increases with nuclear number A as $\langle k_t^2 \rangle = 2Q_s^2 \propto A^{\frac{1}{3}} \text{GeV}^2$. The transverse momentum distribution peaks at $k_t^2 = Q_s^2$ and then decreases towards small k_t, vanishing at zero transverse momentum. We call this dynamical phenomena "supersaturation". A similar behavior for the unintegrated gluon distribution function of nucleus was also derived by the evaluation of the BFKL equation in the nucleus [4]. Supersaturation is quite different from saturation where growth of the gluon density slows down at small transverse momenta cf. [17]. The dynamical origin of supersaturation at small k_t is the dipole-nucleus cross section for large dipoles, which is reduced due to multiple scattering.

III. PRODUCED GLUONS AFTER ONE COLLISION IN HOT INTERACTION AREA

Having the unintegrated gluon density of the nuclei, we calculate the production of gluons and quarks after one collision. To include the intrinsic k_t effects, we adopt the phenomenological k_t-kick model used in previous calculations of hard photon and hadron production [19–21]. Following Ref. [20], we write the cross section for hard collision as

$$\frac{d\sigma(b, p_T)}{dp_T} = \int d^2k_T S(b; k_T) \frac{d\sigma(p_T')}{dp_T'}, \tag{13}$$

where b is the impact parameter of the nucleus-nucleus collision. The differential cross section $\frac{d\sigma(p_T')}{dp_T'}$ is identified as the standard LO QCD predictions for the $2 \rightarrow 2$ processes without intrinsic k_t effects, where the final produced parton would have the transverse momentum p_T'. Due to the kick k_t from the sum of the transverse momenta for the two incident partons,

the real final transverse momentum $\vec{p}_T = \vec{p}'_T + \vec{k}_T$. The averaging function $S(b; k_T)$ reflects the intrinsic k_t effects from the incident partons, which depend on the impact parameter b of the two nuclei, and can be obtained from the unintegrated gluon distribution functions calculated in the previous section. Since the intrinsic gluon distribution functions of the two nuclei depend separately on the locations b_1 and b_2 of the event relative to each nuclear center, we first derive the differential averaging function depending on b_1 and b_2, from Eq. (11),

$$S(b_1, b_2; k_T) = \int \frac{d^2 q_{1T}}{\pi} \frac{d^2 q_{2T}}{\pi} \frac{q_{1T}^2}{(Q_{s1}^2)^2} e^{-\frac{q_{1T}^2}{Q_{s1}^2}} \frac{q_{2T}^2}{(Q_{s2}^2)^2} e^{-\frac{q_{2T}^2}{Q_{s2}^2}} \delta^{(2)}(\vec{q}_{1T} + \vec{q}_{2T} - \vec{k}_T), \qquad (14)$$

where b_1, b_2, and b satisfy the relation $\vec{b}_1 - \vec{b}_2 = \vec{b}$, and Q_{s1}^2, Q_{s2}^2 have the following forms,

$$Q_{s1}^2 = 2T_A(b_1) \times C(0, s), \qquad Q_{s2}^2 = 2T_B(b_2) \times C(0, s). \qquad (15)$$

Since the rest of the integrand the differential mini jet cross section $\frac{d\sigma(p'_T)}{dp'_T}$ does not depend on b_1, b_2, we can integrate Eq. (14) over b_1 and b_2, and obtain a normalized averaging function only depending on b,

$$S(b; k_T) = \frac{\int d^2 b_1 d^2 b_2 T_A(b_1) T_B(b_2) S(b_1, b_2; k_T) \delta^{(2)}(b_1 - b_2 - b)}{\int d^2 b_1 d^2 b_2 T_A(b_1) T_B(b_2) \delta^{(2)}(b_1 - b_2 - b)}. \qquad (16)$$

The above averaging function $S(b; k_T)$ is normalized to unity after integration over k_t. In Fig. 2, we plot this quantity as a function of k_t for different impact parameters b. This figure shows that for more central collisions (smaller b), there is a stronger effect from intrinsic gluon transverse momenta k_t .

From the above formulas, we derive the number of gluons produced in the first collision of nuclei $A + B$ at impact parameter b, applying an infrared cut off p_0 on the produced gluons.

$$N_{AB}(b) = T_{AB}(b)\sigma_{hard}(b, p_0), \qquad (17)$$

where

$$T_{AB}(\vec{b}) = \int d^2 b_1 T_A(\vec{b} - \vec{b}_1) T_B(\vec{b}_1), \qquad (18)$$

$$\sigma_{hard}(b, p_0) = \int_{p_T \geq p_0} dp_T d^2 k_T S(b; k_T) \frac{d\sigma(p'_T)}{dp'_T}. \qquad (19)$$

7

We find that if we neglect the intrinsic k_t effects (setting $S = \delta^{(2)}(k_T)$ in the above equation), we return back to the results in QCD-improved parton model based on the collinear factorization approach [7]. However, for high energy nuclear collisions, we can not neglect these intrinsic k_t effects, which enhance the cross section significantly at a given infrared cut off p_0.

IV. SATURATION OF PRODUCED GLUONS AND INCLUSIVE CROSS SECTION

For central collision ($b = 0$) of identical nuclei A+A with radius R_A, the interaction area of the two nuclei is identical to their transverse size πR_A^2. Assuming the radius of each produced gluon with transverse momentum p_0 to be $1/p_0$, we have saturation for an infrared cut off $p_0 = p_s$ when the produced quanta fill the transverse interaction area πR_A^2. All gluons with momenta smaller than the saturation momenta fuse into gluons with a total momentum larger than the saturation momentum. They are not realistic endproducts for the application of local parton hadron duality to the minijet cross section. So, for central collision, we have the following saturation condition,

$$N_{AA}(p_0 = p_s, b = 0)\frac{\pi}{p_s^2} = T_{AA}(0)\sigma_{hard}(p_s)\frac{\pi}{p_s^2} = \frac{\pi R_A^2}{\beta}. \tag{20}$$

The parameter β takes care of some modification of this simple geometrical picture which can be estimated from the evolution equation including gluon gluon fusion [5] or from [6] and is expected to be around $2 - 3$. More realistic may be a simulation of classical Yang-Mills theory which gives $\beta = 1.4 - 2.0$ [18,22].

We extend the above saturation equation to any arbitrary impact parameter b of the two nuclei,

$$N_{AA}(p_0 = p_s, b)\frac{\pi}{p_s^2} = T_{AA}(b)\sigma_{hard}(p_s(b); b)\frac{\pi}{p_s(b)^2} = \frac{F(b)}{\beta}, \tag{21}$$

where $F(b)$ is the interaction area for $b > 0$. From the geometry of the collision at arbitrary

8

impact parameter b and taking into account the realistic nuclear density profiles of two nuclei, we have the following form for the function $F(b)$:

$$F(b) = \int d^2 b_1 d^2 b_2 (1 - e^{-T_A(b_1)\sigma_{in}})(1 - e^{-T_A(b_1)\sigma_{in}})\delta^{(2)}(b_1 - b_2 - b), \qquad (22)$$

where σ_{in} is the inelastic cross section for proton-proton scattering. In our calculations, we use $\sigma_{in} = 35$, 39, 45mb for $\sqrt{s} = 56$, 130, $200GeV$, respectively. In the limit of sharp-edged nuclear density, this area function will lead to the normal area function of two incident nuclei at impact parameter b

$$F(b) \rightarrow 2\left[R_A^2 arccos(\frac{b}{2R_A}) - \frac{b}{2}\sqrt{R_A^2 - b^2/4}\right].$$

Naturally, the saturation momentum becomes a function of the impact parameter $p_s = p_s(b)$. Having determined the saturation scale $p_s(b)$ from Eq. (21), we plot in Fig. 3 the numerical results for p_s as a function of b for three typical energies at BNL RHIC, $\sqrt{s} = 56$, 130, and $200GeV$, where we set $\beta = 1.8$. From this figure, we can see that the saturation scale p_s increases with collision energy. For central collision ($b = 0$), $p_s = 1.2GeV$ at $\sqrt{s} = 56GeV$, increases to $p_s = 1.3GeV$ at $\sqrt{s} = 130GeV$, and to $p_s = 1.35GeV$ at $\sqrt{s} = 200GeV$.

It is important to differentiate between the saturation scales $Q_s(b_1), Q_s(b_2)$ of intrinsic virtual gluons and the saturation scale $p_s(b)$ of produced gluons. The intrinsic saturation scale is a property of each individual cold nucleus and is defined at the local impact parameter in each nucleus. It parameterizes the intrinsic gluon distribution functions in both nuclei from which the averaging function $S(b, k_T)$ is derived. The saturation scale for the produced gluons p_s is a property of the interacting system of the two nuclei and depends on the nucleus nucleus impact parameter b.

Our results show only a weak dependence of p_s on b which is not so dramatic as found in ref. [10]. Furthermore, the saturation scale p_s in our model is larger than $1GeV$ for a wide range of b. We note that the intrinsic saturation scale Q_s for the gluon distribution in each individual nucleus (15), however, is sensitive to the cylindrical distance b' of the center of the nucleus. In Fig. 3 we show both saturation scales for comparison.

With the saturation scale $p_s(b)$ determined from Eq. (21) we can calculate the number of partons produced after the first collision of $A + B$, from which we can further estimate the charged particle multiplicity [8,7,10]. In Fig. 4 we plot the quantity $\frac{dN_{ch}}{d\eta}/(0.5N_{part.})$ as a function of $N_{part.}$. The number of participants $N_{part.}(b)$ in an A+A collision can be calculated using

$$N_{part.} = 2 \int d^2b_1 T_A(b_1)(1 - e^{-T_A(b_2)\sigma_{in}}).\tag{23}$$

The charged particle multiplicity $\frac{dN_{ch}}{d\eta}$ is related to the parton number produced by the first collision $\frac{dN_{ch}}{d\eta} = \frac{2}{3}\frac{dN}{d\eta}$. To take into account the difference of rapidity and the pseudo-rapidity, we include another factor 0.9 for $\frac{dN}{d\eta} = 0.9\frac{dN}{dy}$ [7,10], which can be calculated from above formulas. From Fig. 4, we see that our predictions on centrality dependence of charged particle multiplicity agree well with the PHENIX data as well as the PHOBOS data except few data points associated with very peripheral collisions, for which the saturation mechanism may not be valid any more.

As a final remark, we note that in [10], quite different from our global saturation approach discussed above, a local saturation condition was introduced for every b_1 and b_2 in each nucleus. If the so determined local $p_s(b_1, b_2)$ is getting too small, an additional cut off is implemented in ref. [10] such that $p_s(b_1, b_2) \geq 0.5$ GeV. This local saturation approach leads to a stronger discrepancy for peripheral collisions than our model cf. Fig 4 and Fig. 4 of Ref. [3]. However, to finally settle this issue, we need more experimental observables and data as suggested in [23].

V. CONCLUSIONS

In this paper, we have calculated the minijet production in $A - A$ collisions at RHIC, including the enhancement from intrinsic transverse momenta of the incident gluons. We derived the unintegrated gluon distributions of cold nuclei and found "super saturation"; the number density of gluons vanishes at zero transverse momentum and has a maximum at the

intrinsic saturation scale Q_s. We differentiate between this gluon saturation scale Q_s inside both nuclei *before* the collision and the saturation scale p_s of produced gluons *after* the first collision between the nuclei. To obtain the saturation scale p_s, we apply the saturation criterion in the central rapidity region, where the produced parton number $\frac{dN}{dy}$ times their individual size π/p_s^2 must not exceed the area $F(b)$ of the two interacting nucleus. Intrinsic transverse momentum of the incident partons increases the number of produced gluons (i.e., the production cross section) at the same cut off, and then leads to a higher saturation scale $p_s \approx 1.5\text{GeV}$ than the scale found without intrinsic k_t. Finally, we find that our numerical results on the centrality dependence of the charged particle multiplicity agree well with the experimental PHENIX and PHOBOS data, which support the saturation scheme we used in this paper.

We note as a final remark, that it is also very important to directly determine the intrinsic transverse momentum scale Q_s for large nuclei. For this purpose we propose to measure "monojet" production at RHIC , in which the final state only contains one large p_T jet without any other large p_T balancing jets. By triggering on produced particles in the projectile and target fragmentation regions with a summed high transverse momentum in one azimuthal hemisphere, one may select minijets with transverse momentum in the opposite azimuthal hemisphere which come from $2 \rightarrow 1$ processes in the central region. In principle one can thereby test the intrinsic saturation scale Q_s which is characteristic for isolated nuclei and also accessible in electron nucleus scattering. The same configuration of monojet production was also suggested in [24] to search the jet quenching effects in high energy parton production. The difference between these two approaches and the experimental accessible will be discussed in the future studies.

REFERENCES

[1] B. B. Back *et al.* [PHOBOS Collaboration], Phys. Rev. Lett. **85**, 3100 (2000) [hep-ex/0007036].

[2] K. H. Ackermann *et al.* [STAR Collaboration], nucl-ex/0009011.

[3] K. Adcox *et al.* [PHENIX Collaboration], nucl-ex/0012008.

[4] M. A. Braun, hep-ph/0010041; Eur. Phys. J. **C16**, 337 (2000).

[5] L. Gribov, E. M. Levin, and M. G. Ryskin, Phys. Reports **100**, 1 (1983); A. H. Mueller and J. Qiu, Nucl. Phys. **B268**, 427 (1986).

[6] J. P. Blaizot and A. H. Mueller, Nucl. Phys. **B289**, 847 (1987).

[7] K. J. Eskola, K. Kajantie, P. V. Ruuskanen and K. Tuominen, Nucl. Phys. **B570**, 379 (2000) [hep-ph/9909456].

[8] Yu. L. Dokshitzer, V. A. Khoze, A. H. Mueller, and S. I. Troya, in *Basics of perturbative QCD*, Paris 1991, pp. 189.

[9] X. Wang and M. Gyulassy, nucl-th/0008014, Phys. Rev. Lett. **86**, 3496 (2001).

[10] K. J. Eskola, K. Kajantie and K. Tuominen, hep-ph/0009246.

[11] D. Kharzeev and M. Nardi, nucl-th/0012025.

[12] see for example, J. R. Forshaw and D. A. Ross, *QCD and the Pomeron*, Cambridge University Press, Cambridge, England, 1996.

[13] H. G. Dosch, T. Gousset, G. Kulzinger and H. J. Pirner, Phys. Rev. D **55**, 2602 (1997) [hep-ph/9608203].

[14] K. Golec-Biernat and M. Wusthoff, Phys. Rev. D **59**, 014017 (1999) [hep-ph/9807513].

[15] B. Z. Kopeliovich, A. Schafer and A. V. Tarasov, Phys. Rev. D **62**, 054022 (2000) [hep-ph/9908245].

[16] K. J. Eskola, V. J. Kolhinen and C. A. Salgado, Eur. Phys. J. **C9**, 61 (1999) [hep-ph/9807297].

[17] A. H. Mueller, Nucl. Phys. **B558**, 285 (1999) [hep-ph/9904404]; A. H. Mueller, Nucl. Phys. **B572**, 227 (2000) [hep-ph/9906322]; Y. V. Kovchegov and A. H. Mueller, Nucl. Phys. **B529**, 451 (1998) [hep-ph/9802440].

[18] L. McLerran and R. Venugopalan, Phys. Rev. D **49**, 2233 (1994) [hep-ph/9309289]; Phys. Rev. D **49**, 3352 (1994) [hep-ph/9311205]; Phys. Rev. D **50**, 2225 (1994) [hep-ph/9402335].

[19] J. Huston, E. Kovacs, S. Kuhlmann, H. L. Lai, J. F. Owens and W. K. Tung, Phys. Rev. D **51**, 6139 (1995) [hep-ph/9501230]; L. Apanasevich *et al.*, Phys. Rev. D **63**, 014009 (2001) [hep-ph/0007191].

[20] H. Lai and H. Li, Phys. Rev. D **58**, 114020 (1998) [hep-ph/9802414].

[21] X. Wang, Phys. Rev. Lett. **81**, 2655 (1998) [hep-ph/9804384]; Phys. Rev. C **61**, 064910 (2000) [nucl-th/9812021].

[22] A. Krasnitz and R. Venugopalan, Phys. Rev. Lett. **84**, 4309 (2000) [hep-ph/9909203]; hep-ph/0007108.

[23] M. Gyulassy, I. Vitev and X. N. Wang, Phys. Rev. Lett. **86**, 2537 (2001) [nucl-th/0012092].

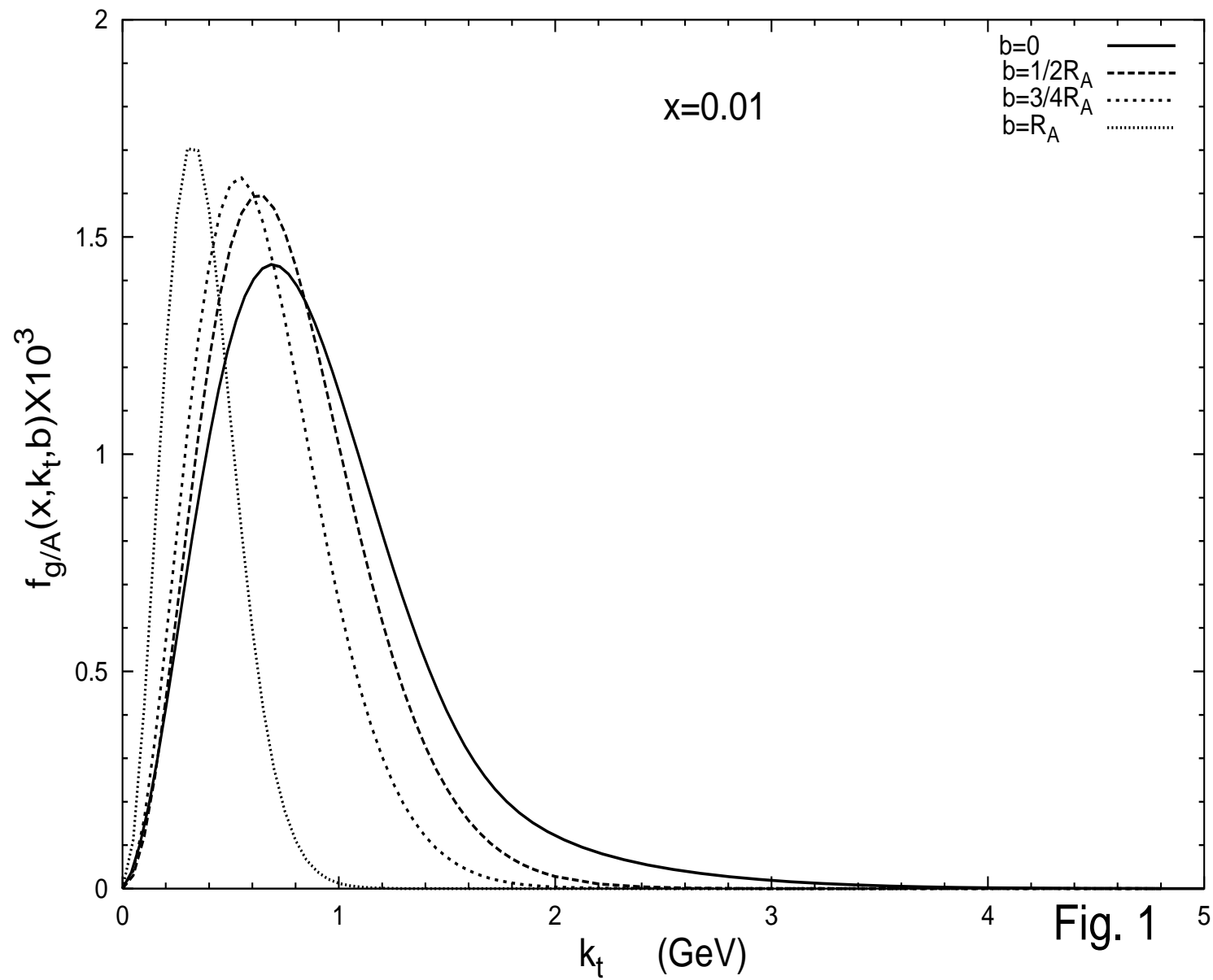[24] M. Pluemer, M. Gyulassy and X. N. Wang, Nucl. Phys. A **590**, 511C (1995).
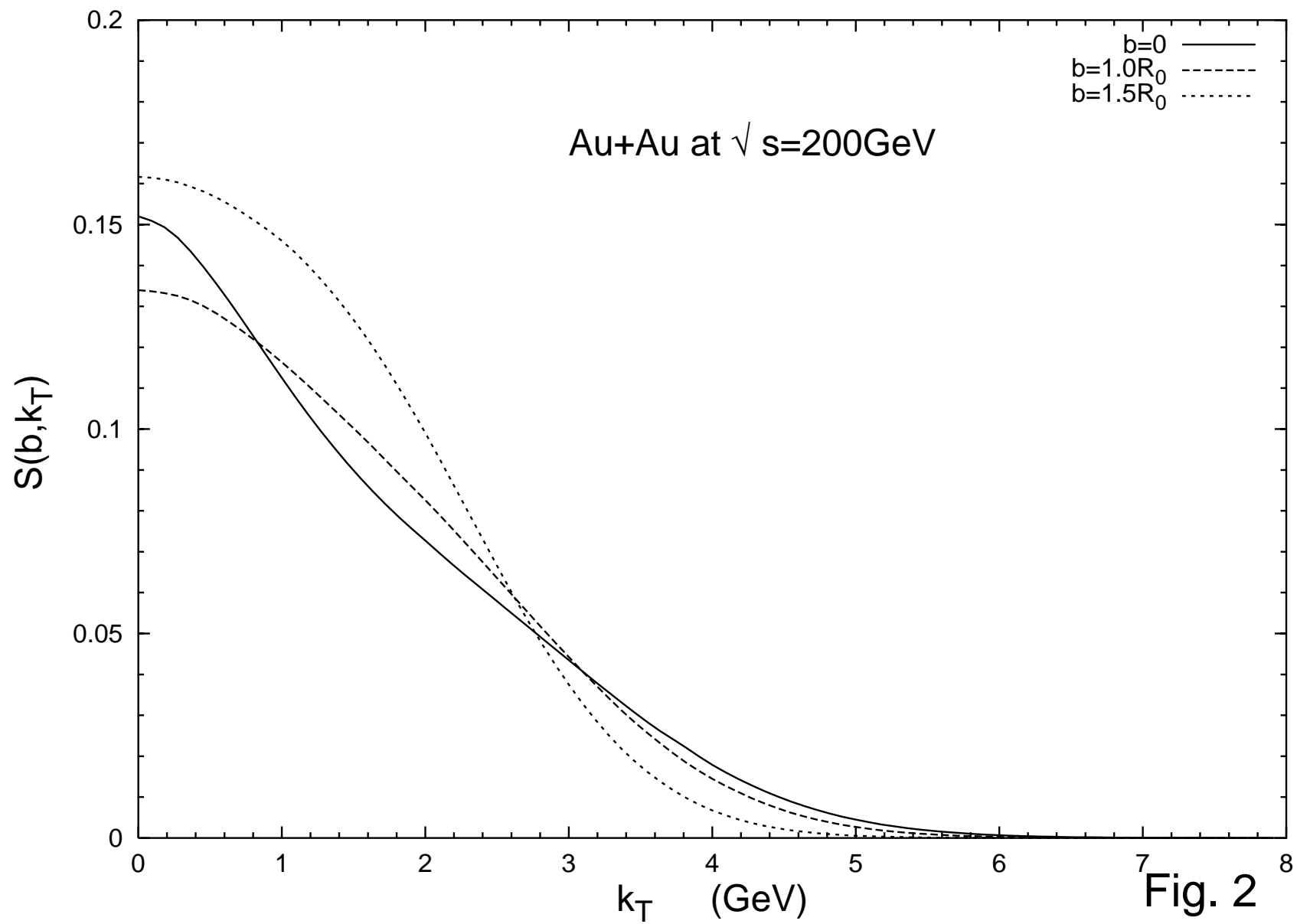
Figure Captions

FIG.1. The double differential gluon distribution $f_{g/A}(x, k_t, b)$ for Au($A = 197$, $R_A = 6.37\ fm$) at $x = 10^{-2}$ as a function of k_t [GeV] at different cylindrical distances ($b = 0$, $1/2R_A$, $3/4R_A$, R_A) from the central axis of the nucleus. The maxima of these distributions are at $k_t = Q_s \approx 0.96 GeV$, $0.90 GeV$, $0.76 GeV$, $0.46 GeV$ for these four cases respectively.

FIG. 2. The averaging function $S(b; k_T)$ vs k_T for different nucleus-nucleus impact parameters b shows that intrinsic transverse momentum kicks k_t with larger k_T are more numerous for central collisions at $b = 0$ than for peripheral collisions with large b.

FIG. 3. The saturation scale p_s in GeV is shown as a function of b for three different energies $\sqrt{s} = 56 GeV$, $130 GeV$, $200 GeV$. We also plot the intrinsic saturation scale Q_s ($x = 0.01$) as a function of b' for the individual nuclei before collision, where b' is the cylindrical distance from the central axis of the nucleus. In contrast to p_s, Q_s is a more strongly varying function of b'.

FIG. 4. The theoretical normalized charged particle multiplicity $[dN_{ch}/d\eta]/(0.5N_{part.})$ as a function of the number of participants $N_{part.}$ is shown for the theory with intrinsic gluon transverse momentum k_t (full line) and without k_t averaging effects (dashed line). The crosses mark the experimental PHENIX ($+$) and PHOBOS ($\times$) data.
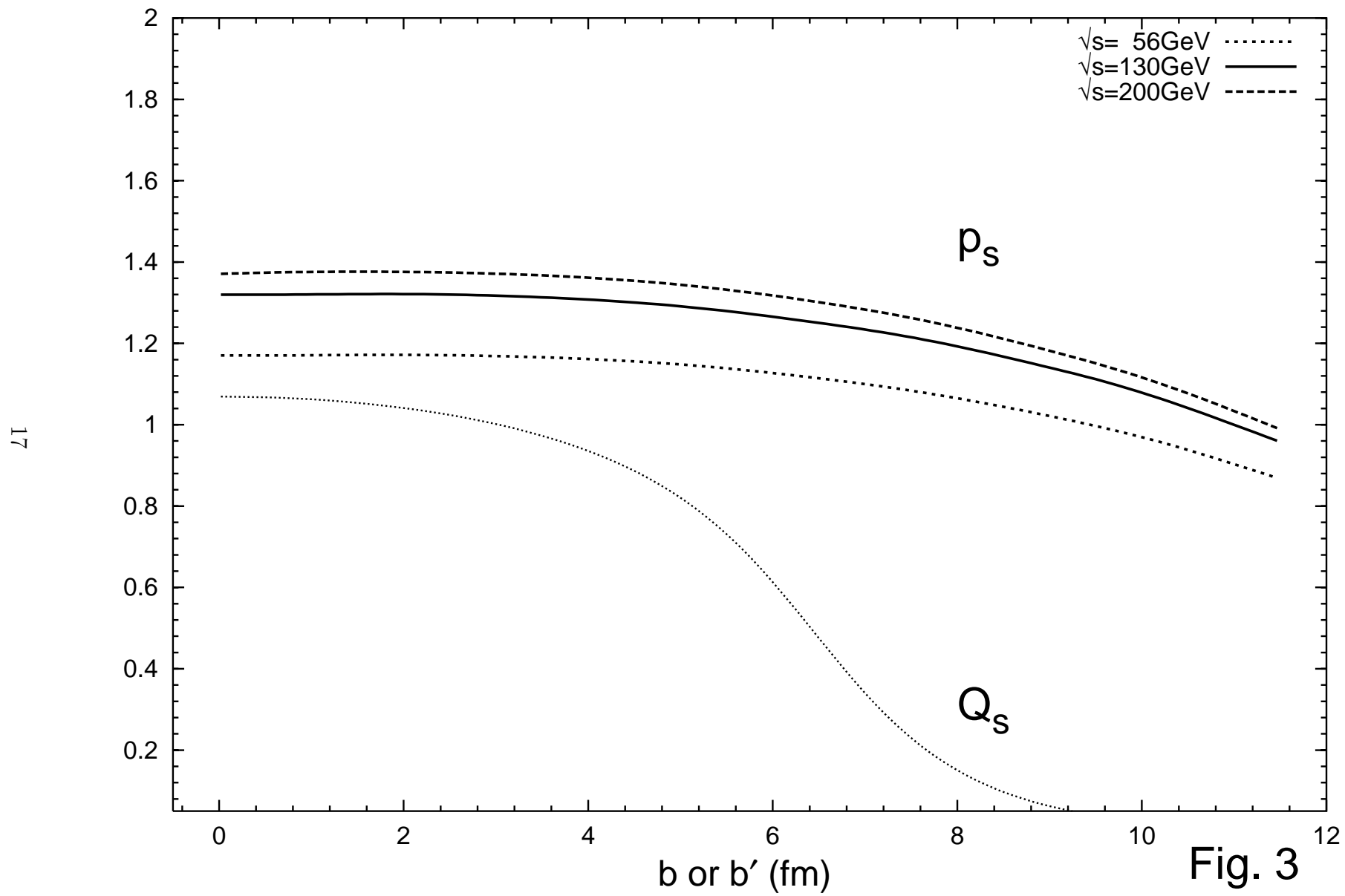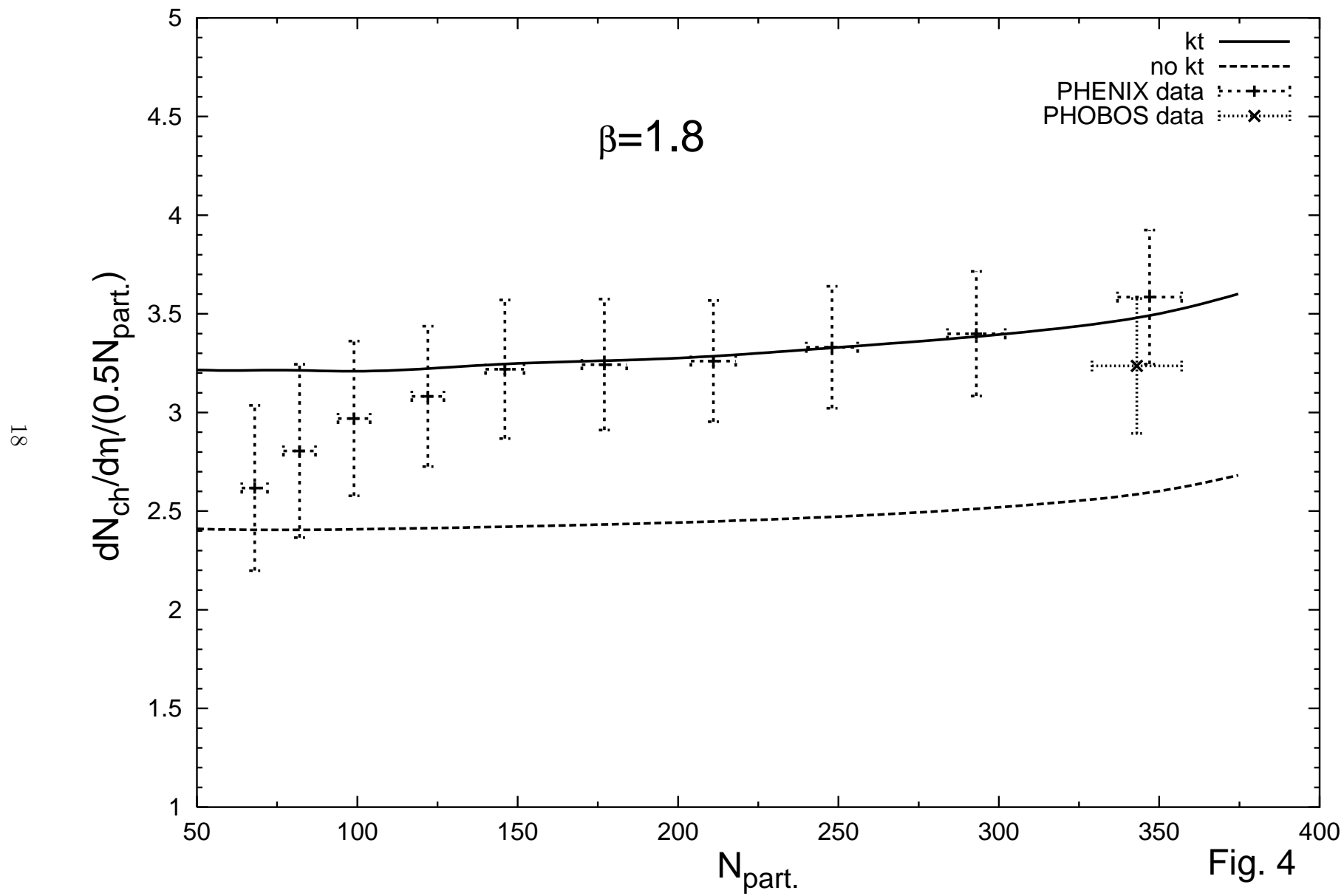
Fig. 1

Au+Au at $\sqrt{s}=200$GeV

Fig. 2

16

Fig. 3

Fig. 4